Crystal Structure of Exotype Alginate Lyase Atu3025 from *Agrobacterium tumefaciens*[*]

Akihito Ochiai[‡], **Masayuki Yamasaki**[§], **Bunzo Mikami**[§], **Wataru Hashimoto**[‡], and **Kousaku Murata**[‡1]

From the ‡*Laboratory of Basic and Applied Molecular Biotechnology and the* §*Laboratory of Applied Structural Biology, Graduate School of Agriculture, Kyoto University, Uji, Kyoto 611-0011, Japan*

Alginate, a major component of the cell wall matrix in brown seaweeds, is degraded by alginate lyases through a β-elimination reaction. Almost all alginate lyases act endolytically on substrate, thereby yielding unsaturated oligouronic acids having 4-deoxy-L-erythro-hex-4-enepyranosyluronic acid at the nonreducing end. In contrast, *Agrobacterium tumefaciens* alginate lyase Atu3025, a member of polysaccharide lyase family 15, acts on alginate polysaccharides and oligosaccharides exolytically and releases unsaturated monosaccharides from the substrate terminal. The crystal structures of Atu3025 and its inactive mutant in complex with alginate trisaccharide (H531A/ΔGGG) were determined at 2.10- and 2.99-Å resolutions with final *R*-factors of 18.3 and 19.9%, respectively, by x-ray crystallography. The enzyme is comprised of an α/α-barrel + anti-parallel β-sheet as a basic scaffold, and its structural fold has not been seen in alginate lyases analyzed thus far. The structural analysis of H531A/ΔGGG and subsequent site-directed mutagenesis studies proposed the enzyme reaction mechanism, with His[311] and Tyr[365] as the catalytic base and acid, respectively. Two structural determinants, *i.e.* a short α-helix in the central α/α-barrel domain and a conformational change at the interface between the central and C-terminal domains, are essential for the exolytic mode of action. This is, to our knowledge, the first report on the structure of the family 15 enzyme.

Carbohydrate-active enzymes such as glycoside hydrolases, polysaccharide lyases, glycosyl transferases, and carbohydrate esterases are categorized into more than 200 families based on amino acid sequences in the Carbohydrate-Active enZYmes (CAZy) data base (1). Polysaccharide lyases (PLs)[2] are classified into 21 PL families and they play an important role in degrading acidic polysaccharides such as polygalacturonan, rhamnogalacturonan, alginate, chondroitin, hyaluronan, heparin, heparan, and xanthan. These lyases commonly recognize uronic acid residues in polysaccharides, catalyze β-elimination, and produce unsaturated saccharides with C=C double bonds at nonreducing terminal uronate residues.

Alginate, produced by brown seaweeds as a major component of the cell wall matrix, is a linear polysaccharide composed of α-L-guluronate (G) and its C5 epimer β-D-mannuronate (M). Three blocks, such as poly-α-L-guluronate (poly(G)), poly-β-D-mannuronate (poly(M)), and heteropolymeric random sequences (poly(MG)), constitute the alginate polymer (2). The alginate degradation pathway has been characterized in some bacteria, virus, and abalone. In the bacterium *Sphingomonas* sp. strain A1, alginate is directly incorporated into the cytoplasm by the cell surface pit, periplasmic binding proteins, and ATP-binding cassette transporter. The incorporated alginate is subsequently depolymerized into unsaturated disaccharides, trisaccharides, and tetrasaccharides through the action of three cytoplasmic endotype alginate lyases, A1-I, A1-II, and A1-III (Fig. 1*A*) (3). The unsaturated oligosaccharides thus formed are finally degraded by the cytoplasmic exotype alginate lyase A1-IV into monosaccharides (4); these are then nonenzymatically converted to α-keto acids, *i.e.* 4-deoxy-L-erythro-5-hexoseulose uronic acids (Fig. 1*B*). An A1-IV homologue Atu3025 is also encoded in the genome of *Agrobacterium tumefaciens*. *A. tumefaciens* cells show significant growth on low molecular weight alginate (average molecular weight 1000), and Atu3025 inducibly expressed in the bacterial cells is prerequisite for degradation of the substrate (5). Family PL-15 A1-IV and Atu3025 function in each host cell as the sole enzymes involved in producing unsaturated monosaccharides; thus, they are essential for alginate metabolism. In other bacteria, virus, and abalone, alginate lyases have been shown to release unsaturated oligosaccharides (6–8). No exotype alginate lyase that release monosaccharides has been reported. Although some polysaccharide lyases, such as polygalacturonate lyases (*Thermotoga maritima* PelA in family PL-1 (9) and *Erwinia chrysanthemi* PelX in family PL-9 (10)), rhamnogalacturonan lyase (*Bacillus subtilis* YesX in family PL-11 (11)), xanthan lyase (*Bacillus* sp. strain GL1 XLY in family PL-8 (12)), and alginate lyases (*Chlorella* virus vAL-1 (13) and *Haliotis discus hannai* HdAlex in family PL-14 (8), and A1-IV and Atu3025 in family PL-15), have previously been identified as exotype enzymes. A1-IV and Atu3025 are distinguished clearly from the other enzymes by a specific character; that is, both are processing-type enzymes that release
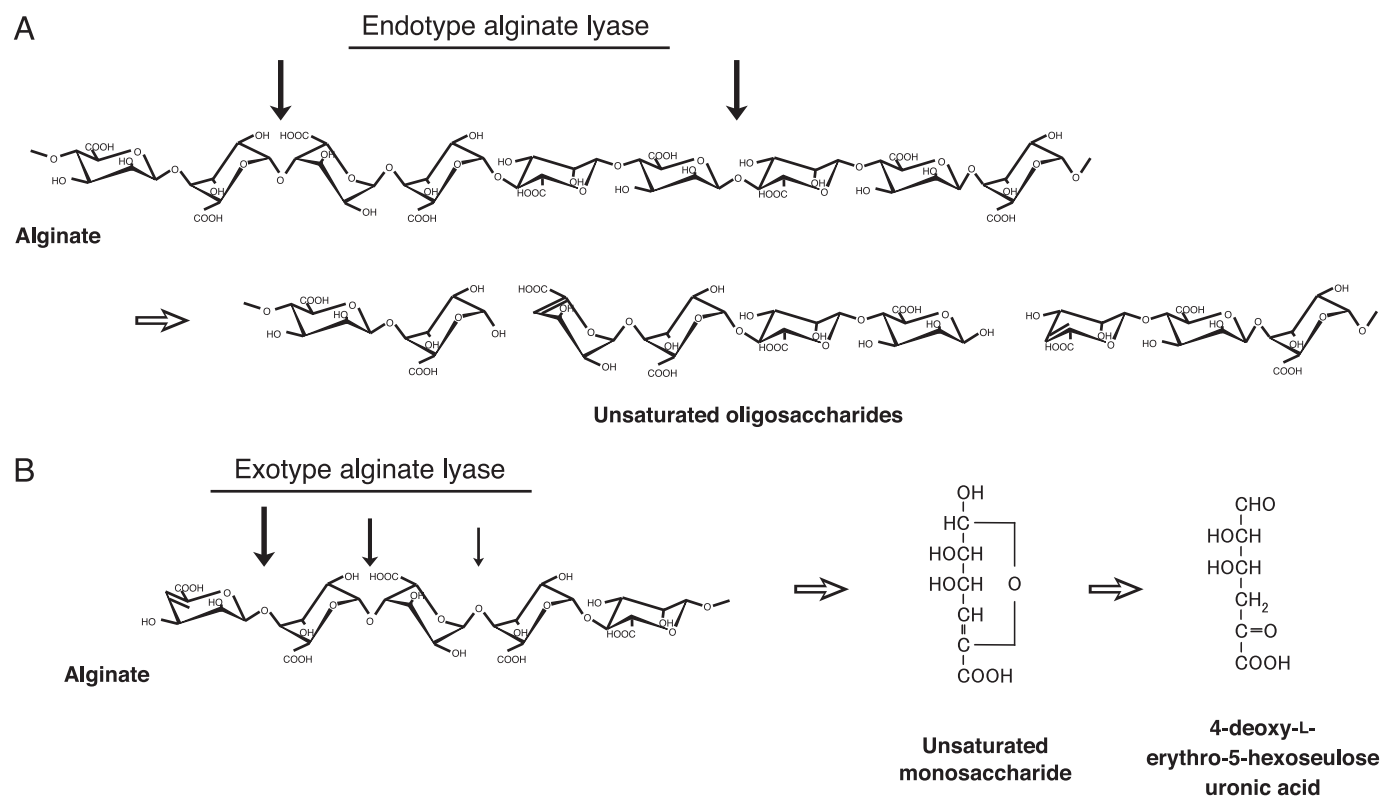
Structure of Exotype Alginate Lyase

FIGURE 1. **Alginate degradation by endotype (*A*) and exotype (*B*) alginate lyases.** *Thick arrows* indicate the cleavage sites for each enzyme against substrate.

unsaturated monosaccharides from the polysaccharide chain (4, 5).

The crystal structures of PLs in 18 families have been determined, and the structure and functional relationships of enzymes such as pectin lyase in family PL-1 (14); pectate lyases in families PL-2, PL-3, and PL-10 (15–17); alginate lyases in families PL-5, PL-7, and PL-14 (13, 18, 19); rhamnogalacturonan lyases in families PL-4 and PL-11 (20, 21); chondroitin lyases in families PL-6 and PL-8 (22); hyaluronan lyases in families PL-8 and PL-16 (23, 24); heparin lyases in families PL-13 and PL-21 (25, 26); and xanthan lyase in family PL-8 (12) have been demonstrated. On the other hand, no structural information on family PL-15 alginate lyases has been accumulated, and the enzyme mechanism for releasing unsaturated monosaccharides from the polysaccharide main chain remains to be clarified. This article deals with the determination of crystal structures of family PL-15 Atu3025 and its complex with unsaturated alginate trisaccharide through x-ray crystallography, and identification of the active site structure responsible for substrate recognition and exolytic reaction.

EXPERIMENTAL PROCEDURES

Materials—Sodium alginate (polymerization degree, around 650; viscosity, 1,000 cp) from *Eisenia bicyclis* was purchased from Nacalai Tesque. DEAE-Toyopearl 650M was purchased from Tosoh; HiLoad 26/10 Q-Sepharose High Performance, HiLoad 16/60 Superdex 200pg, and Superdex Peptide 10/300 GL from GE Healthcare.

Enzyme and Protein Assays—The assay for alginate lyase was conducted as follows. The enzyme was incubated at 30 °C for 5 min in a reaction mixture (1 ml) consisting of 0.05% sodium alginate and 50 mM Tris-HCl (pH 7.5). The reaction mixture was heated at 100 °C for 5 min to terminate the reaction, and the amount of unsaturated uronic acids produced in the reaction mixture was determined by the thiobarbituric acid method (27). In each assay, the enzyme was stable and the reaction products were confirmed to increase proportionally with time and enzyme concentration in the reaction mixture. Enzyme activity was determined by measuring the increase in absorbance at 548 nm, resulting from the condensation of β-formylpyruvic acid with thiobarbituric acid ($\epsilon = 2.9 \times 10^4$/M cm). One unit of enzyme activity was defined as the amount of enzyme required to liberate 1 μmol of β-formylpyruvic acid per minute at 30 °C. For site-directed mutants, the enzyme assay was done as follows. To estimate the specific activity of the mutants, a large amount of the enzyme was incubated at 30 °C for 60 min in a reaction mixture (1 ml) consisting of 0.05% unsaturated β-D-mannuronate disaccharide (ΔMM) and 50 mM Tris-HCl (pH 7.5). One unit of enzyme activity was defined as the amount of enzyme required to degrade 1 μmol of ΔMM/min at 30 °C. Quantification of the residual ΔMM was performed using high performance liquid chromatography. An ÄKTA purifier (GE Healthcare) equipped with a Superdex Peptide 10/300 GL was used for high performance liquid chromatography analysis. Reaction products were eluted at a flow rate of 0.5 ml/min with 10 mM potassium phosphate (pH 7.0) and detected by measuring the absorbance at 235 nm on the basis of C=C double bonds in the ΔMM. Protein content was determined by the

Bradford method (28), with bovine serum albumin as the standard.

Expression and Purification of Atu3025 and Its Derivative with Selenomethionine—Protein expression and purification of Atu3025 were conducted as described previously (5). The DNA fragment encoding the complete sequence of the Atu3025 gene (GenBank number AE007870) with the original stop codon was ligated with pET21b. Thus, the polypeptide expressed from the resultant plasmid (pET21b/Atu3025) was not fused to the histidine-tagged sequence. An overexpression system for the Atu3025 derivative with selenomethionine (SeMet Atu3025) was also constructed in *Escherichia coli* cells. Unless specified otherwise, all purification procedures were performed at 0–4 °C. *E. coli* B834(DE3) cells harboring pET21b/Atu3025 were grown in 6 liters of minimal medium (29) (1.0 liter/flask) implemented with 25 mg of selenomethionine/liter. The cells were collected by centrifugation at $6,000 \times g$ for 5 min, washed with 20 mM Tris-HCl (pH 7.5) supplemented with 0.5 mM dithiothreitol (DTT), and resuspended in the same buffer. After ultrasonic disruption of cells at 9 kHz for 20 min, the clear solution obtained on centrifugation at $20,000 \times g$ for 20 min was used as the cell extract. After an overnight dialysis against 20 mM Tris-HCl (pH 7.5) supplemented with 0.5 mM DTT, the cell extract was applied to a DEAE-Toyopearl 650M column (2.5×10 cm) previously equilibrated with 20 mM Tris-HCl (pH 7.5) supplemented with 0.5 mM DTT. The absorbed proteins were eluted with a linear gradient of NaCl (0–700 mM) in 20 mM Tris-HCl (pH 7.5) supplemented with 0.5 mM DTT (200 ml), and 4-ml fractions were collected every 4 min. Fractions containing SeMet Atu3025, which were eluted between 300 and 500 mM NaCl, were combined and dialyzed overnight against 20 mM Tris-HCl (pH 7.5) supplemented with 0.5 mM DTT. The dialysate was applied to a HiLoad 26/10 Q-Sepharose High Performance column (2.6×10 cm) previously equilibrated with 20 mM Tris-HCl (pH 7.5) containing 300 mM NaCl and 0.5 mM DTT. The absorbed proteins were eluted with a linear gradient of NaCl (300–500 mM) in 20 mM Tris-HCl (pH 7.5) supplemented with 0.5 mM DTT (150 ml), and 4-ml fractions were collected every 1 min. Fractions containing SeMet Atu3025, which were eluted between 380 and 420 mM NaCl, were combined and applied to a HiLoad 16/60 Superdex 200 pg column (1.6×60 cm) previously equilibrated with 20 mM Tris-HCl (pH 7.5) containing 0.15 M NaCl and 0.5 mM DTT. The proteins were eluted with the same buffer (120 ml), and 2-ml fractions were collected every 2 min. These two purification steps, such as Q-Sepharose High Performance and Superdex 200 pg, were done by the using ÄKTA purifier at room temperature. Fractions containing SeMet Atu3025 were combined and dialyzed overnight against 20 mM Tris-HCl (pH 7.5), and used as the purified SeMet Atu3025. The purified SeMet Atu3025 had the same N-terminal amino acid sequence as Atu3025, with a calculated molecular mass of 87,871 Da from the predicted amino acid sequence (776 residues).

Site-directed Mutagenesis—To replace Arg[199], His[311], Tyr[365], Trp[467], and His[531] by Ala, Ala, Phe, Ala, and Ala, respectively, Atu3025 mutants were constructed using a QuikChange site-directed mutagenesis kit (Stratagene). The plasmid pET21b/Atu3025 (5) was used as a PCR template, and the follow-ing oligonucleotides were used as primers: R199A, sense 5′-CGT-GTCGCCACGCTCTGGG<u>C</u>G<u>C</u>AGATGTATATAGACTGC-3′, and antisense 5′-GCAGTCTATATACATCTGC<u>G</u>C<u>C</u>CAGA-GCGTGGCGACACG-3′; H311A, sense 5′-GTCTTTCCCTAT-GACAGC<u>G</u>C<u>T</u>GCGGTGCGCTCGCTTTC-3′, and antisense 5′-GAAAGCGAGCGCACCGCA<u>G</u>C<u>G</u>CTGTCATAGGGAAA-GAC-3′; Y365F, sense 5′-GCGGAAGGTCCGCATTT<u>C</u>TGGA-TGACCGGCATG-3′, and antisense 5′-CATGCCGGTCATCC-AG<u>A</u>AATGCGGACCTTCCGC-3′; W467A, sense 5′-GCCTTT-TACAATTACGGC<u>G</u>C<u>G</u>TGGGACCTCAACTTCGACGATC-3′, and antisense 5′-GATCGTCGAAGTTGAGGTCCCACGC-GCCGTAATTGTAAAAGGC-3′; H531A, sense 5′-CTTACGG-TTCGCTCAGC<u>G</u>C<u>C</u>CAGTCACGGCGACCAG-3′, and anti-sense 5′-CTGGTCGCCGTGACTG<u>G</u>C<u>G</u>CTGAGCGAACCGT-AAG-3′ (mutations are underlined). Mutations were confirmed by DNA sequencing with an automated DNA sequencer (model 377; Applied Biosystems). Expression and purification of the mutants were conducted using the same procedures as for Atu3025.

Crystallization and X-ray Diffraction—Atu3025 (20 mg/ml) was crystallized by sitting-drop vapor diffusion on Linbro tissue culture plates as described previously (30). The condition most suitable for Atu3025 crystallization was determined to be a mixture of 80 mM Tris-HCl (pH 8.5), 24% (w/v) polyethylene glycol 4,000, 0.16 M magnesium chloride, and 20% (v/v) glycerol. The SeMet Atu3025 was crystallized under the same condition as the native Atu3025 crystal. A crystal for the site-directed mutant (H531A) in complex with alginate trisaccharide (ΔGGG) was prepared by sitting drop vapor diffusion on Intelli plates (Veritas). The droplet (2 μl) was prepared by mixing 1 μl of the protein solution with 1 μl of the reservoir solution and equilibrated at 20 °C against 0.05 ml of reservoir solution. The H531A/ΔGGG complex crystal appeared through sparse matrix screening using a Crystal Screen Cryo kit from Hampton Research in about six months. The condition most suitable for H531A/ΔGGG crystallization was determined to be a mixture of 85 mM HEPES-Na (pH 7.5), 17% (w/v) polyethylene glycol 4,000, 8.5% (v/v) isopropyl alcohol, 15% (v/v) glycerol, and 10 mM ΔGGG. The crystal on a nylon loop (Hampton Research) was placed directly in a cold nitrogen gas stream at −173 °C, and x-ray diffraction images of the crystal were collected at −173 °C under a nitrogen gas stream with a Jupiter 210 CCD detector and synchrotron radiation of wavelength 1.000 Å at the BL-38B1 station of SPring-8 (Hyogo, Japan). During data collection for single-wavelength anomalous diffraction analysis using the SeMet Atu3025 crystal, the synchrotron radiation wavelength was adjusted to 0.9792 Å. The wavelength was defined from XAFS measurement of the SeMet Atu3025 crystal. The 240 diffraction images (total 240°) with 1.0° oscillation were collected as a consecutive series of datasets. Diffraction data were processed using the HKL2000 program package (31). Data collection statistics are summarized in Table 1.

Structure Determination and Refinement—The crystal structure of Atu3025 was solved by the single-wavelength anomalous diffraction method using the SeMet Atu3025 crystal. Selenium sites and initial phasing were determined by the SOLVE program (32). Density modifications (solvent flattening and histogram matching) were done using the program RESOLVE

TABLE 1

Data collection and refinement statistics

	Atu3025	SeMet Atu3025	H531A/ΔGGG
Space group	$P1$	$P2_12_12_1$	$P2_12_12_1$
Unit cell parameters (Å, °)	$a = 64.2, b = 68.2, c = 108.9\ \alpha = 78.3, \beta = 89.3, \gamma = 88.6$	$a = 107.8, b = 108.1, c = 301.1$	$a = 81.8, b = 99.7, c = 109.2$
Data collection			
Wavelength (Å)	1.0000	0.9792	1.0000
Resolution limit (Å)	50.0–2.10 (2.17–2.10)[a]	50.0–3.40 (3.52–3.40)[a]	50.0–2.99 (3.11–2.99)[a]
Total reflections	260,783	341,167	77,140
Unique reflections	104,273	49,442	18,590
Redundancy	2.5 (1.2)	3.8 (3.7)	4.2 (4.2)
Completeness (%)	96.7 (88.7)	95.0 (89.8)	99.5 (99.9)
$I/\delta\ (I)$	5.3 (2.3)	5.2 (4.1)	11.2 (4.9)
R_{merge} (%)	5.8 (24.8)	12.5 (35.0)	9.9 (36.1)
Refinement			
Final model			
Protein residues	764, 763 (molecules A, B)		766
Water	1,067		62
Chloride ions	2		
Sugar (ΔGGG)			1
Resolution limit (Å)	40.9–2.11 (2.16–2.11)		37.9–2.99 (3.07–2.99)
Used reflections	95,821 (6,080)		17,479 (1,221)
Completeness (%)	96.4 (83.6)		99.0 (94.6)
Average B-factor (Å^2)			
Protein	23.5, 28.7 (molecules A, B)		37.7
Water	33.6		24.6
Chloride ions	19.0		
Sugar (ΔGGG)			48.7
R-factor (%)	18.3 (21.8)		19.9 (28.9)
R_{free} (%)	22.4 (25.4)		26.2 (34.1)
Root mean square deviations			
Bond (Å)	0.007		0.008
Angle (°)	1.04		1.064
Ramachandran plot (%)			
Favored regions	97.1		95.3
Allowed regions	2.9		4.7

[a] Data on the highest shells are given in parentheses.

(33). The initial model was built to consist of 2,812 amino acid residues without side chains through manual modeling and refinement. The Coot program (34) was used for the modification of the initial model. The 50.0–2.10-Å resolution dataset was truncated with the CCP4 program package (35) and used for subsequent refinement. The H531A/ΔGGG crystal was solved by molecular replacement using the Molrep program in the CCP4 program package with the native Atu3025 structure as a reference model. Initial rigid body refinement and several rounds of restrained refinement against the dataset were done using the Refmac5 program (36). Water molecules were incorporated where the difference in density exceeded 3.0 σ above the mean and the $2F_o − F_c$ map showed a density of more than 1.0 σ. The structure of the enzyme-sugar complex was refined using the Coot program with the parameter file for gulurononic acid at the PRODRG site. Protein models were superimposed, and their root mean square (r.m.s.) deviations were determined with the LSQKAB program (37), a part of the CCP4 program package. Final model quality was checked with the PROCHECK program (38). Ribbon plots were prepared using the PyMOL program (39). Coordinates used in this work were taken from the RCSB Protein Data Bank (PDB) (40).

RESULTS AND DISCUSSION

Structure Determination and Refined Model Quality—Data collection and refinement statistics are summarized in Table 1. The refined model from the Atu3025 crystal includes 1,527 amino acid residues, 1,067 water molecules, two chloride ions for two protein molecules, designated as Atu3025 molecules A

and B, in an asymmetric unit. 10 amino acid residues ([1]MRP-SAPAISR[10]) in molecule A and 11 amino acid residues ([1]MRP-SAPAISRQ[11]) in molecule B N-terminal, and 2 amino acid residues ([775]QF[776]) C-terminal in each molecule could not be assigned in the $2F_o − F_c$ map possibly due to disorder. The final overall R-factor for the refined model was 18.3% with 95,821 unique reflections within a 40.9–2.11-Å resolution range. The final overall free R-factor calculated with randomly selected 5% reflection was 22.4%. Based on theoretical curves in the plot calculated according to Luzzati (41), the absolute positional error was estimated to be 0.23 Å at a resolution of 2.11 Å. Ramachandran plot analysis (42), in which the stereochemical correctness of the backbone structure is indicated by (ϕ, ψ) torsion angles (43), shows that 97.1% of nonglycine residues are in the favored region and 2.9% are in the allowed regions. Four *cis*-peptides were observed between Glu[27] and Pro[28], Asn[37] and Pro[38], His[139] and Pro[104], and Tyr[349] and Ser[350] residues in each molecule.

Overall Structure—The overall structure (Fig. 2, *A–C*) and topology of the secondary structure elements (Fig. 2*D*) indicate that alginate lyase Atu3025 consists of three globular domains: N-terminal small β-sheet domain, central α-domain, and C-terminal β-sheet domain. The N-terminal small β-sheet domain consists of 106 amino acid residues from Gln[11] to Ile[116] and is composed of two antiparallel β-sheets consisting of seven β-strands (S1 to S7). The central α-domain consists of 364 amino acid residues from Arg[128] to Asp[491] and is constituted by 15 α-helices (HA1 to HA12 and H1 to H3). The three helices,
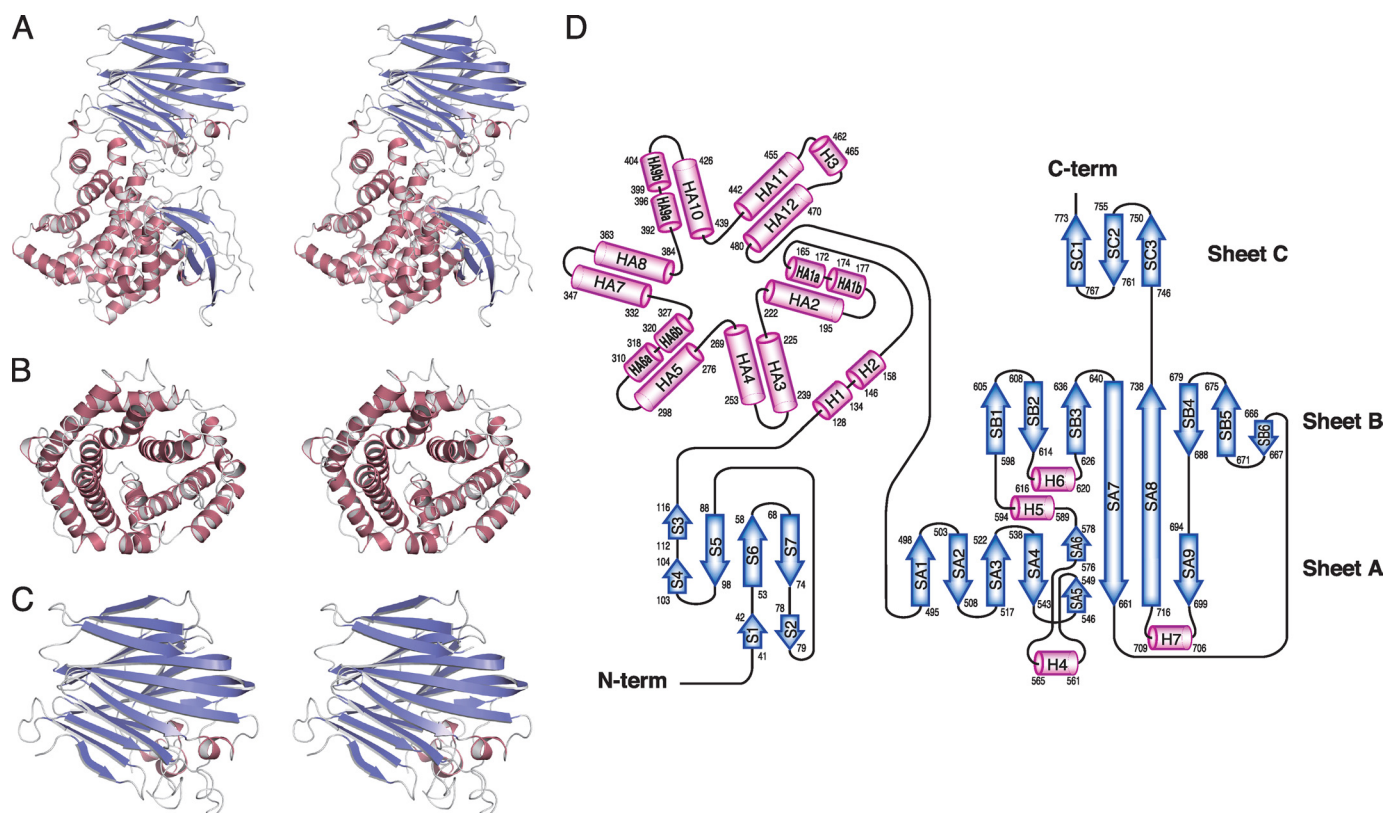
FIGURE 2. **Structure of Atu3025.** *A*, overall structure (stereodiagram). *B*, central α-domain (stereodiagram). *C*, C-terminal β-domain (stereodiagram). *D*, topology diagram. β-Sheets are shown as *blue arrows*, and helices are shown as *pink cylinders*.

such as HA1, HA6, and HA9, are divided into two segments, HA1a (amino acid residues 165–172) and HA1b (174–177), HA6a (310–318) and HA6b (320–327), and HA9a (392–396) and HA9b (399–404), respectively. There are one or two additional residues (HA1, Val[173]; HA6, Val[319]; and HA9, Thr[397] and Gly[398]) whose oxygen atom has no hydrogen bond with the nitrogen atom of a paired residue. The 12 helices, HA1 to HA12, contribute to the formation of an α_6/α_6-barrel structure with a deep cleft (Fig. 2, *B* and *D*) and are connected by short and long loops in a nearest neighbor, up-and-down pattern. This arrangement is described as a "twist α/α-barrel" with six inner α-helices (HA2, HA4, HA6, HA8, HA10, and HA12), which are oriented in roughly the same direction, and six outer α-helices (HA1, HA3, HA5, HA7, HA9, and HA11) running in the opposite direction. The two helices, H1 and H2, are connected between the N-terminal small β-sheet and α_6/α_6-barrel domains. The other short helix H3 is adjoined to the long helices. The C-terminal β-sheet domain consists of 279 amino acid residues from Leu[495] to Pro[773] and is constituted by 18 β-strands (SA1 to SA9, SB1 to SB6, and SC1 to SC3) and four short α-helices (H4 to H7). These β-strands constitute three antiparallel β-sheets (sheet A, SA1-SA9; sheet B, SB1-SB6 and SA7-SA8; and sheet C, SC1-SC3), forming a three-layered β-sheet sandwich structure (Fig. 2, *C* and *D*). Helices H4, H6, and H7 are located between strands SA4 and SA5 in sheet A, SB2 and SB3 in sheet B, and SA8 and SA9 in sheet A, respectively. Helix H5 is positioned between strands SA6 in sheet A and SB1 in sheet B.

TABLE 2
Structure-based homology with Atu3025

Z score	Description	R.m.s. deviation	LALI[a]	PDB code
30.8	Heparinase II protein	3.6	577	2FUQ
18.4	Alginate lyase A1-III	3.7	292	3EVH
15.5	Xanthan lyase	5.4	490	1X1H
15.3	Hyaluronate lyase	5.4	431	1LXM
15.2	Hyaluronate lyase	5.2	446	1OJM
15.0	Chondroitinase AC	5.0	470	1HMW
14.8	Chondroitin AC lyase	3.6	231	1RW9
14.3	Chondroitin ABC lyase I	3.6	219	1HN0
14.0	4-α-Glucanotransferase	5.9	254	1K1X
13.9	Chondroitin sulfate lyase ABC	6.4	504	2Q1F

[a] Total number of equivalenced residues.

Alginate lyases classified into families PL-5, PL-6, PL-7, PL-14, PL-17, PL-18, and PL-20 adopt the α/α-barrel or the β-jelly roll as a basic structural scaffold, demonstrating that the α/α-barrel + anti-parallel β-sheet of family PL-15 Atu3025 is a novel scaffold in the alginate lyases analyzed thus far. Structural homologues of Atu3025 were searched for in the PDB using the DALI program (44). Several proteins such as heparinase II protein (PDB entry 2FUQ, $Z = 30.8$) (26), xanthan lyase (PDB entry 1X1H, $Z = 15.5$) (12), and hyaluronate lyase (PDB entry 1LXM, $Z = 15.3$) (45) were found to exhibit a significant structural homology to overall structure of Atu3025 (Table 2). Because family PL-5 alginate lyase A1-III and family PL-8 and PL-21 chondroitin/heparin lyases are classified into the chondroitin AC/alginate lyase superfamily due to the presence of an α/α-barrel domain in the SCOP data base (46), Atu3025 is regarded as a member of the lyase superfamily.
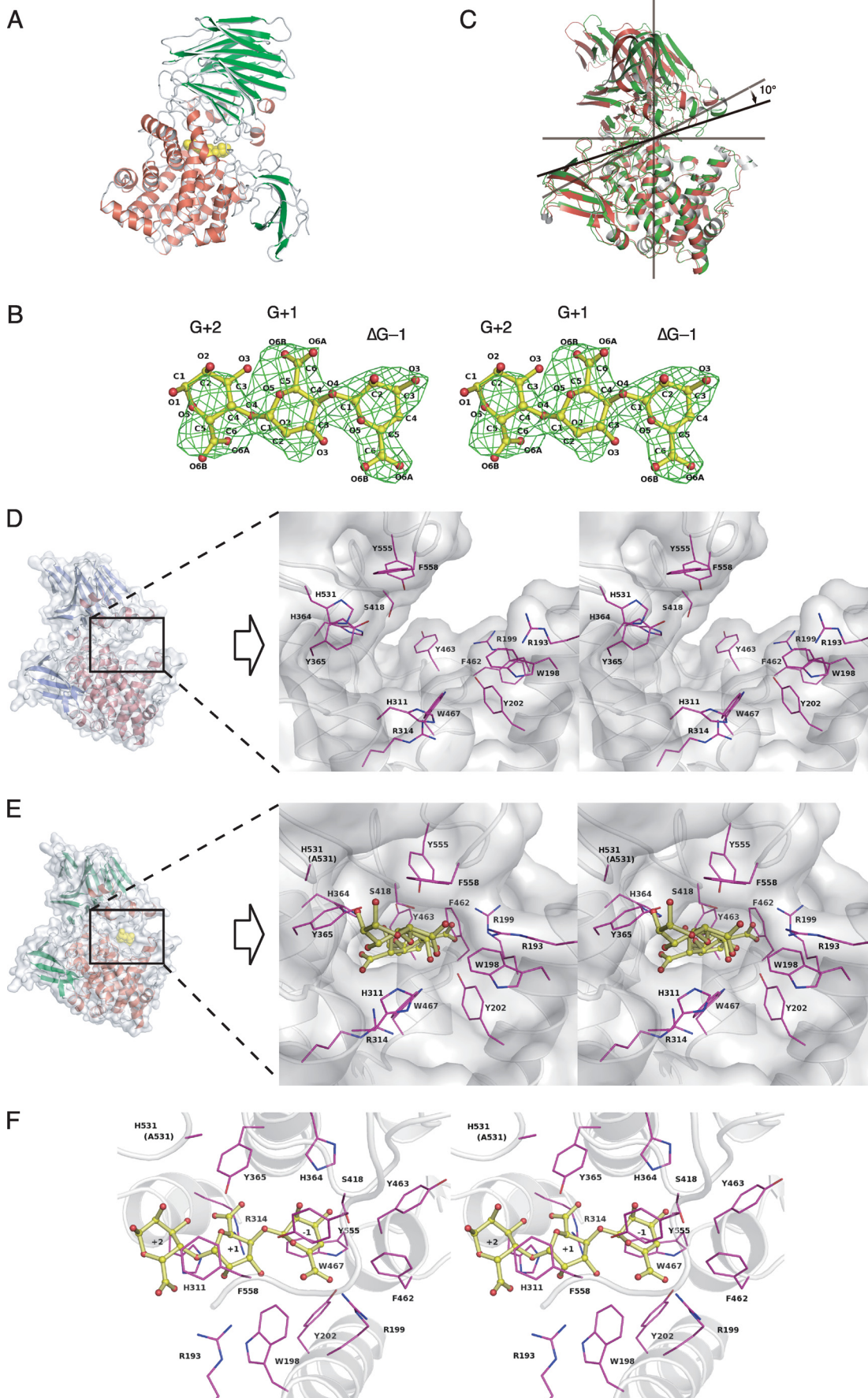
Conformational Change by Substrate Binding—To identify the catalytic residues and structural determinants for the exolytic mode of action in Atu3025, a crystal of H531A/ΔGGG was prepared. His[531] comprises a component of the active pocket, and the mutant H531A shows a significantly lower activity than the wild-type enzyme. Data collection and refinement statistics are summarized in Table 1. The crystal structure of H531A/ΔGGG determined at 2.99-Å resolution consists of 766 amino acid residues, which are derived from an Atu3025 monomer, and one ΔGGG molecule in an asymmetric unit. The ΔGGG molecule was bound to the deep pocket between central α/α-barrel and C-terminal β-sheet domains (Fig. 3A). The nonreducing terminal and central residues of ΔGGG are well fitted in the electron density map with average B-factors of 42.0 and 47.4 Å^2, whereas the reducing terminal residue are poorly fitted (average B-factor of 55.5 Å^2) (Fig. 3B).

The r.m.s. deviation between ligand-free Atu3025 and H531A/ΔGGG complex structures was calculated as 1.59 Å for all residues (764 Cα atoms), indicating that significant conformational changes occur between protein structures with and without ΔGGG. Fig. 3C shows the superimposition of ligand-free Atu3025 and H531A/ΔGGG. The protein structures have been aligned by use of only the central α/α barrel domain (amino acid residues from Arg[128] to Asp[491]). The C-terminal β-sheet domain of Atu3025 can adopt two different conformations through a rigid-body rotation of ~10°. This hinge bending motion was observed in the plane formed at the interface of the α/α-barrel and C-terminal β-sheet domains. ΔGGG is included in the pocket-like active center, causing the conformational rearrangement (Fig. 3E). Several amino acid residues such as Arg[193], Trp[198], Arg[199], Tyr[202], Glu[254], His[311], Arg[314], His[364], Tyr[365], Ser[418], Phe[462], Tyr[463], Trp[467], His[531], Tyr[555], and Phe[558] are arranged around the active pocket. Structure comparison of ligand-free Atu3025 and H531A/ΔGGG demonstrates that the side chain of Phe[462] is turned away and interacts with Ser[418], which is positioned at the opposite side of the active pocket (Fig. 3, D and E), suggesting that Phe[462] plays an important role in forming the pocket. Enzyme flexibility as seen in Atu3025 has been reported in family PL-8 hyaluronate lyase from *Streptococcus pneumoniae* (47); this flexibility is essential to construct the active center for enzymes with an α/α-barrel + anti-parallel β-sheet topology.

Active Site Structure—The crystal structure of H531A/ΔGGG revealed the binding mode of the substrate ΔGGG molecule to the active cleft (Fig. 3F). Subsites are labeled so that −n represents the nonreducing terminus and n the reducing terminus, and cleavage occurs between the −1 and +1 sites (48). Atu3025 depolymerizes alginate exolytically, releasing monosaccharides from the nonreducing end of the polymer through a β-elimination reaction. Based on the location of the nonreducing terminus residue of ΔGGG in the deepest spot of the active pocket, the saccharides are considered to be positioned at

TABLE 3
Interactions between Atu3025 and ΔGGG

Sugar	Hydrogen bond (≤3.5Å)			C-C contact (≤4.5Å)	
	/ Atom	Protein / Atom	Distance (Å)	/ Atom	Protein / Atom(s)
G+2	/ O2	Ser-530 / Oγ	3.4	/ C2	Ser-310 / Cβ
	/ O3	Ser-310 / Oγ	3.0	/ C3	Ser-310 / Cβ
		His-311 / Nε2	3.4		His-311 / Cδ2, Cε1
	/ O4	His-311 / Nε2	3.3	/ C4	His-311 / Cε1
					Phe-558 / Cε1, Cε2, Cζ
				/ C5	Phe-558 / Cε1, Cε2, Cζ
				/ C6	Phe-558 / Cδ2, Cε2, Cζ
G+1	/ O2	Glu-254 / Oε2	3.5	/ C1	His-311 / Cε1
		His-311 / Nε2	3.2		Phe-558 / Cγ, Cδ1, Cδ2, Cε1, Cε2, Cζ
	/ O5	Tyr-365 / Oη	3.0	/ C2	Trp-198 / Cζ2, Cη2
	/ O6A	Tyr-365 / Oη	3.5		His-311 / Cε1
	/ O6B	Ser-310 / Oγ	2.9		Phe-558 / Cβ, Cγ, Cδ1
		His-311 / Nε2	3.1	/ C3	Trp-198 / Cζ2, Cη2
		Arg-314 / Nη1	3.3		Phe-558 / Cβ, Cδ1
				/ C5	His-311 / Cδ2, Cε1
					Tyr-365 / Cζ
				/ C6	His-311 / Cδ2
					Tyr-365 / Cε2, Cζ
G−1	/ O2	His-364 / Nε2	2.8	/ C1	Trp-467 / Cζ2, Cη2
	/ O3	His-364 / Nε2	3.5	/ C2	Ser-418 / Cβ
	/ O5	Tyr-555 / Oη	3.3		Trp-467 / Cζ2, Cη2
	/ O6A	Arg-199 / Nε	2.9	/ C3	Ser-418 / Cβ
		Arg-199 / Nη2	2.9		Trp-467 / Cδ2, Cε2, Cζ2, Cη2
		Tyr-202 / Oη	2.8	/ C4	Ser-418 / Cβ
	/ O6B	Arg-199 / Nη2	3.1		Phe-462 / Cε1
					Trp-467 / Cε2, Cζ2, Cη2
				/ C5	Trp-198 / Cη2
					Ser-418 / Cβ
					Phe-462 / Cε1
					Trp-467 / Cζ2
					Tyr-555 / Cε2
				/ C6	Trp-198 / Cζ3, Cη2
					Arg-199 / Cζ
					Phe-462 / Cδ1, Cε1
					Tyr-555 / Cε2

subsites −1, +1, and +2. Therefore, the constituent guluronic acid residues of ΔGGG are designated as ΔG−1, G+1, and G+2 from the nonreducing end. Several amino acid residues are responsible for binding to ΔGGG (Table 3, Fig. 3F). ΔG−1 is accommodated at subsite −1 through seven hydrogen bonds by four residues, Arg[199], Tyr[202], His[364], and Tyr[555], and 26 carbon-carbon (C-C) contacts by six residues, Trp[198], Arg[199], Ser[418], Phe[462], Trp[467], and Tyr[555]. Residue Trp[467] interacts with the pyranose ring of ΔG−1 through a stacking interaction by 12 C-C contacts. At subsite +1, seven hydrogen bonds by five residues, Glu[254], Ser[310], His[311], Arg[314], and Tyr[365], and 23 C-C contacts by four residues, Trp[198], His[311], Tyr[365], and Phe[558], are formed between G+1 and protein. At subsite +2, G+2, the reducing terminal residue of ΔGGG, is hydrogen bonded to three residues, Ser[310], His[311], and Ser[530], and there are 14 C-C contacts by three residues, Ser[310], His[311], and Phe[558]. Phe[558] is partially parallel to the pyranose ring of both G+1 and G+2, indicating that the residue undergoes a partially stacking interaction with the sugar ring of these two residues. Positively charged residues such as Arg[199] and Arg[314] are supposed to be crucial for binding acidic polysaccharides and/or neutralizing the negative charge of the carboxyl groups in ΔG−1 and G+1. A multiple sequence alignment of family PL-15 exotype alginate lyases using the ClustalW program is shown in Fig. 4. Atu3025 shows a significant sequence identity of 55.0% with

FIGURE 3. **Active site structure of Atu3025.** *A,* overall structure of H531A/ΔGGG. *B,* electron density of the ΔGGG molecule in the active pocket by the omit map ($F_o − F_c$) calculated without ΔGGG and countered at 3.0 σ. *C,* superimposition of ligand-free Atu3025 (*red*) and H531A/ΔGGG (*green*). *D,* surface model and active site structure (*inset,* stereodiagram) of the ligand-free Atu3025. *E,* surface model and active site structure (*inset,* stereodiagram) of H531A/ΔGGG. *F,* residues in the H531A/ΔGGG structure interacting with the ΔGGG molecule in the active pocket. Amino acid residues and ΔGGG molecule are shown by colored elements: oxygen atom, *red,* carbon atom, *pink* in amino acid residues, and *yellow* in the ΔGGG molecule; nitrogen atom, *deep blue.* Characters in *panel B* indicate the saccharide number and its atoms. Characters in *panels D–F* indicate the subsite and amino acid residue numbers.

```
                                            S1              S6              S7          S2        S5
Atu3025  1  MRPSAPAISRQTLLDEPRPGSLTIGYEPSEEAQPTENPPRFSWLPDIDDGARYVLRISTDPGFTDKKTLVFEDLAWNFFTPDEALPDGHY  90
A1-IV       ----------MKKLEQPQSADMTIRYFP-DSDTLTENPPRFLWLPELDSQARYAVRVVSDAG----KETVFGDIQHNFFRPDVTLTPGSY
            . *:*:....:** * * .  ******* ***::*. ***.:*.:* .*    * ** *: *** ** :*. * *

              S5        S4        S3              H1                  H2            HA1a     HA1b
Atu3025  91 HWCYALWDQKSATAHSNWSTVRSFEISEALPKTPLPGRSARHAAAQTSHPRLWLNSEQLSAFADAVAKDPNHCGWAEFYEKSVEPWLERP 180
A1-IV       TWSYALWDAAAGKVDSDWSSPRSFVLPADAPAVPGMRHKERYACDMTHPRLWLSQSEATALGKSVATDPDHCKWANFMAKSVTPWMSRE
            *.***** :::..*.*::**: *** :.   * .*  :. *:*.:: :******...: :*:..:**.**:** **:* *** **:.*

                       rvvvvvvvvvvvvvvvvvvvv HA2 vvvvvvvvvvv    vvvvvvv HA3 vvvvvvvvv        vvvvvv HA4 vvvvvvv
Atu3025 181 VMPEPQPYPNNTRVATLWRQMYIDCQEVIYAIRHLAIAGRVLGRDDLLDASRKWLLAVAAWDTKGATSRAYNDEAGFRVVVALAWGYDWL 270
A1-IV       IIAEPQPYPNNKRTPALWRKMYIDCQEVIYAIRHLAIAGRVLGDAAMTARAKEWLLAVAAWDVRGPTCRDYNDEAAFRIAAALAWGYDWL
            ::.********.*..*:***:**:***************...: ::*********.**.*** :*** :*****:*********

              vvvvvvvvvvvvv HA5 vvvvvvvvvvv          vvvv HA6a vvvv  vvvv HA6b vvvv    vvvvv HA7 vvvvv
Atu3025 271 YDHLSEDERRTVRSVLLERTREVADHVIAHARIHVFPYDSFAVRSLSAVLTPACIALQGESDEAGEWLDYTVEFLATLYSPWAGTDGGWA 360
A1-IV       HDELSDIERANVRESLTVRTREVANHVINRAKIHIFPYDSFAVRSISSVLVPCSIVLLGEVPEAQKWLDYSIDFYDAIYPPWGGVDGGWA
            :*.**: ** .**  . ** .*****.***:.*:**.****** ***:** * * ** *.  *** .:** * :*** **.*.*****

                        vvvvvvvvvvvvv HA8 vvvvvvvvvvvv      vvvv HA9a vvvv  vvvv HA9b vvvv          vvvvvvvvvvvvv HA10 vvvvvvvvvvvv  vvvv HA11 vvvv
Atu3025 361 EGPHYWMTGMAYLIEAANLIRSYIGYDLYQRPFFQNTGRFPLYTKAPGTRRANFGDDSTLGDLPGLKLGYNVRQFAGVTGNGHYQWYFDH 450
A1-IV       EGPHYWMTAMAYFTEAANLVLKYFKHDLYKRPFFQSTGWFPLYTKAPDTRRACFGDDSTLGDLPCLKVGYNLRQFAGVTGNPYFQWYFEE
            ********.*** :*****:  *:.:***:*****.**:*********.****.******:********.*.********** ::****::.

               vvvv HA11 vvvv      H3       vvvvv HA12 vvvvv              SA1             SA2             SA3                      SA4
Atu3025 451 IKADATGTEMAFYNYGWWDLNFDDLVYRHDYPQVEAVSPADLPALAVFDDIGWATIQKDMEDPDRHLQFVFKSSPYGSLSHSHGDQNAFV 540
A1-IV       VCRNDPGTEMEFYNYGWWDLNFDDVQYLHDFPHIEAKAPSDIDTVKYFGDVGWVALQRHMDKPDQHIQFLTKASDFGSISHSHGDQGAFL
            : :  .**** ***************: * **:*: ** **: *.::*.*.**.*:* *::*:**:**: *:* :***:*********.**:

                SA4     SA5           H4          SA6              H5        SB1          SB2       H6          SB3
Atu3025 541 LYAHGEDLAIQSGYYVAFNSQMHLNWRRQTRSKNAVLIGGKGQYAEKDKALARRAAGRIVSVEEQPGHVRIVGDATAAYQVANPLVQKVL 630
A1-IV       LYGYGEDLAIQSGYMIGFGTTMHKEWRRLTKSKNAILIDGKGQYSGSNKAECLKAQGHVLEVGTRNGAHFISLDPTDAYKAEVPYLTRYR
            **. *********** :.* ..**: ***.*.*****:**.****:..**.* *.* *: ** :*. *:* * *.*:* ** :: :  *

                                                                       SB4
                                                                     (arrow)
                SB3        SA7            SB6      SB5         SB4           SA9         H7        SA8
Atu3025 631 RETHFVNDSYFVIVDEVECSEPQELQWLCHTLGAPQTGRSSFRYNGRKAGFYGQFVYSSSGGTPQISAVEGFPDIDPKEFEGLDIHHHVCA 720
A1-IV       RDIHFVHDRFFVIVDDVELEQDGSVQWLMHTFKPCELGSQVFRYHGDKAGLNGEFVYCSSGPVSIENTVSYANIDQSEVEGLPPQSTLVA
            *:.***:*.:*****:**  . . .*** **:   .* *.*** *.****::*:***.***  .* .* .*:**:* **** * ** * *

                              SA8                SC3        SC2          SC1
Atu3025 721 TVPAATRHRLVTLLVPYSLKEPKRIFSFIDDQGFSTDIYFSDVDDERFKLSLPKQF 776
A1-IV       STGAARRHTLVTLLTPYALSAPLRVFHFNDDQGFSTNLYFQDGNNEMYTITLPKPF
            :. ***.**.****** ** . *  :* * ******::** *.:*  * * **** *
```
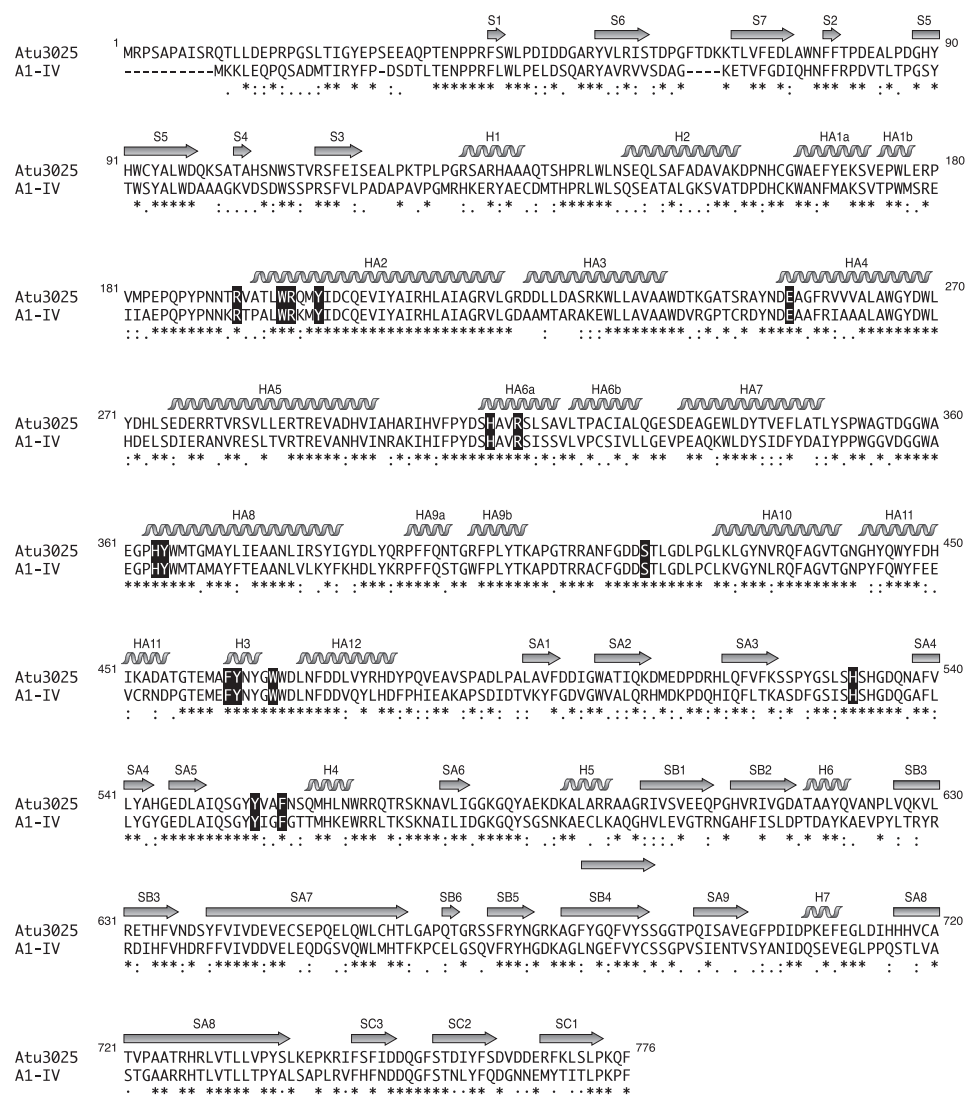
FIGURE 4. **Alignment of amino acid sequences of family PL-15 alginate lyase.** Atu3025, alginate lyase from *A. tumefaciens* strain C58 (GenPept accession number AAL43841); A1-IV, alginate lyase from *Sphingomonas* sp. strain A1 (GenPept accession number BAB03319). Amino acid sequences were aligned using the ClustalW program. Identical and similar amino acid residues in these alginate lyases are denoted by *asterisks* and *dots*, respectively. Secondary structure elements of Atu3025 are as shown *above*. Amino acid residues interacting with ΔGGG are highlighted in *black*.

TABLE 4
Specific activity of wild-type and Atu3025 mutants

Enzyme	Specific activity[a]	Relative activity
	milliunits/mg	*%*
Wild-type	1,140	100
R199A	49	4.3
H311A[b]		
Y365F	3.4	0.30
W467A	0.12	0.011
H531A	5.1	0.45

[a] The value of wild-type is taken as 100%.
[b] The activity of the H311A mutant is too weak to determine the specific activity.

carboxylate anion, (ii) a general base catalyst abstracts the proton from C-5 of the uronic acid residue, and (iii) a general acid catalyst donates the proton to the glycoside bond to be cleaved. To identify the role of Atu3025 residues in the active site, we constructed the mutants, R199A, H311A, Y365F, W467A, and H531A, in which Arg[199], His[311], Tyr[365], Trp[467], and His[531] were replaced by Ala, Ala, Phe, Ala, and Ala, respectively. These residues for mutation were supposed to play an important role in recognizing the acidic polysaccharide and/or catalyzing the enzyme reaction based on the structure of H531A/ΔGGG. The mutants were overexpressed in *E. coli* cells and purified to homogeneity. Their specific activities were determined as follows (Table 4). In all mutants, especially H311A and W467A, the enzyme activity significantly decreased. Various amino acid residues are reported to act as a catalytic base or acid in PL families. Although Arg in families PL-1 and PL-10 (17), Lys in family PL-9 (50), Tyr in families PL-5 (19), and PL-8 (22), and His in family PL-7 (18) function as a catalytic base, Tyr in families PL-5 (19), PL-7 (18), and PL-8 (22) function as a catalytic acid. In the family PL-5 alginate lyase A1-III from *Sphingmonas* sp. strain A1, Tyr[246] is considered to act as both a catalytic base and acid (19). On the other hand, the family PL-7 alginate lyase A1-II′ from *Sphingmonas* sp. strain A1 adopts His[191] and Tyr[284] as the catalytic base and acid (18), respectively. These catalytic His and Tyr residues well conserved in families PL-5 and PL-7 correspond to His[311] and Tyr[365] in Atu3025, respectively. Based on the active site structure of H531A/ΔGGG (Fig. 3*F*), the distance between His[311] and C5 of G+1 was calculated as 3.4 Å, and between Tyr[365] and O4 of G+1 was less than 4.0 Å. Judging from the significant decrease in the specific activity of H311A and Y365F (Table 4), it is plausible that His[311] and Tyr[365] function as a catalytic base and acid, respectively (Fig. 5), as seen in A1-II′ (18). Tyr[555] is also a candidate for a catalytic acid because the distance between Tyr[555] and O4 of G+1 was determined as 4.0 Å (Fig. 5), although the Tyr residue is not conserved in family PL-15 alginate lyases (Atu3025, A1-IV, and A1-IV′), so far characterized. His[531] is located close enough to interact with the carbohydrate group of G+1, when the residue retains the similar side chain conformation as in the ligand-free Atu3025 (Fig. 3*D*). Due to this struc-
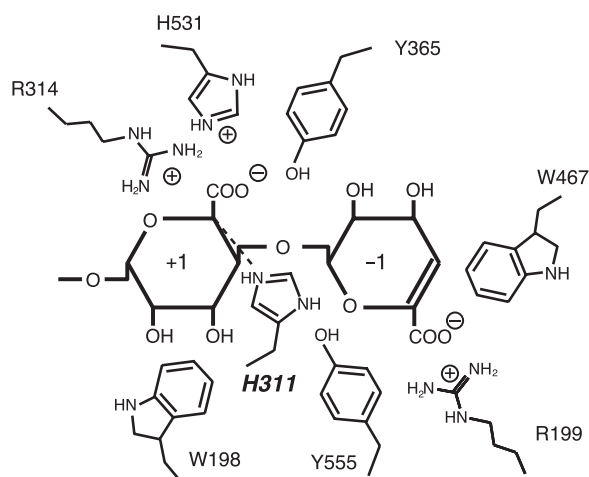
A1-IV from *Sphingomonas* sp. A1. The residues outlined above are completely conserved between the two.

Structural Insights into the Catalytic Reaction and Exolytic Mode of Action—The catalytic reaction of polysaccharide lyases is divided into three steps as follows (49): (i) positively charged residues stabilize or neutralize the negative charge on the C-6

FIGURE 5. **Catalytic center in Atu3025.** The residues surrounding subsites −1 and +1 are represented schematically.

tural feature and low activity of H531A (Table 4), His[531] is supposed to play a major role in stabilizing or neutralizing the negative charge on the carboxylate anion of G+1 (Fig. 5). The reduced activity of R199A indicates that Arg[199] also functions as a stabilizer on the carboxyl group of ΔG-1 as described above. The intrinsic function of each possible catalytic residue should be analyzed through structure determination of the enzyme and substrate complex at higher resolution.

Unlike other polysaccharide lyases, family PL-15 enzymes such as Atu3025 and A1-IV can release unsaturated monosaccharides from polysaccharide. The crystal structure of H531A/ΔGGG shows a part of the structural determinants for the exolytic mechanism. The distinguishing characteristic of Atu3025, namely a pocket-like structure, is observed in the environment surrounding subsite −1. The pocket is formed by two structural determinants, *i.e.* a conformational change at the interface between the central and C-terminal domains and the presence of a short α-helix H3 (Fig. 3, *D* and *E*). Tyr[555] and Phe[558] in the C-terminal β-sheet domain and Phe[462] and Trp[467] around H3 are actually involved in accommodating the substrate (Table 3). At subsite −1, seven hydrogen bonds and 26 C-C contacts are formed between the enzyme and sugar. In particular, Trp[467] forms 12 C-C contacts with ΔG-1 and the mutant W467A showed the significant reduction in the specific activity compared with the wild-type (Table 4), indicating that the residue is essential for recognition of a nonreducing terminal residue of the substrate. This pocket-like structure is not observed in other polysaccharide lyases, even in the family PL-8 and PL-20 enzymes with the α/α-barrel + anti-parallel β-sheet as a basic scaffold. In family PL-8 hyaluronate lyase from *S. pneumoniae* (47), a pocket-like structure is absent in its active site although the conformational change caused by substrate binding has been reported. Some polysaccharide lyases such as rhamnogalacturonan lyase YesX from *B. subtilis* and alginate lyase vAL-1 from *Chorella* virus have been reported to release the unsaturated disaccharide exolytically. Their previous crystallographic studies demonstrated that the steric hindrance at one end of the active cleft and the sugar-binding affinity level in subsites are crucial for the exolytic mode of action of YesX (51) and vAL-1 (13), respectively. Therefore, it is reasonable to presume that

the pocket-like structure is a characteristic of the family PL-15 exotype alginate lyases, which release unsaturated monosaccharides as a sole product, and is essential for recognizing the nonreducing terminal residues of substrate. Based on the above described results, Atu3025 probably adopts the five-step cycle to exhibit the exolytic mode of action as follows: (i) alginate approaches the active site of the "open form" enzyme, (ii) the terminal saccharide of the polymer is accommodated at subsite −1 through the conformational modulation (open/close), (iii) the glycosidic linkage is cleaved in the "closed form," (iv) the enzyme takes the open form to release the product, and (v) the remaining substrate slides along the active site through the conformational modulation (open/close).

Conclusions—This is, to our knowledge, the first report on the structural determination of the family PL-15 enzyme and establishment of a new structural category in alginate lyases involving an α/α-barrel + anti-parallel β-sheet-fold. The active site structure of H531A/ΔGGG and the subsequent site-directed mutational analysis suggest that His[311] and Tyr[365] function as a catalytic base and acid, respectively. Additionally, a pocket-like structure of Atu3025, which is formed by the conformational change at the interface between the central and C-terminal domains, is essential for the exolytic mode of action involved in releasing unsaturated monosaccharides from the polysaccharide main chain.

REFERENCES

1. Cantarel, B. L., Coutinho, P. M., Rancurel, C., Bernard, T., Lombard, V., and Henrissat, B. (2009) *Nucleic Acids Res.* **37,** D233–D238
2. Wong, T. Y., Preston, L. A., and Schiller, N. L. (2000) *Annu. Rev. Microbiol.* **54,** 289–340
3. Yoon, H.-J., Hashimoto, W., Miyake, O., Okamoto, M., Mikami, B., and Murata, K. (2000) *Protein Expr. Purif.* **19,** 84–90
4. Hashimoto, W., Miyake, O., Momma, K., Kawai, S., and Murata, K. (2000) *J. Bacteriol.* **182,** 4572–4577
5. Ochiai, A., Hashimoto, W., and Murata, K. (2006) *Res. Microbiol.* **157,** 642–649
6. Gimmestad, M., Ertesvåg, H., Heggeset, T. M., Aarstad, O., Svanem, B. I., and Valla, S. (2009) *J. Bacteriol.* **191,** 4845–4853
7. Suda, K., Tanji, Y., Hori, K., and Unno, H. (1999) *FEMS Microbiol. Lett.* **180,** 45–53
8. Suzuki, H., Suzuki, K., Inoue, A., and Ojima, T. (2006) *Carbohydr. Res.* **341,** 1809–1819
9. Kluskens, L. D., van Alebeek, G. J., Voragen, A. G., de Vos, W. M., and van der Oost, J. (2003) *Biochem. J.* **370,** 651–659
10. Brooks, A. D., He, S. Y., Gold, S., Keen, N. T., Collmer, A., and Hutcheson, S. W. (1990) *J. Bacteriol.* **172,** 6950–6958
11. Ochiai, A., Itoh, T., Kawamata, A., Hashimoto, W., and Murata, K. (2007) *Appl. Environ. Microbiol.* **73,** 3803–3813
12. Maruyama, Y., Mikami, B., Hashimoto, W., and Murata, K. (2007) *Biochemistry* **46,** 781–791
13. Ogura, K., Yamasaki, M., Yamada, T., Mikami, B., Hashimoto, W., and Murata, K. (2009) *J. Biol. Chem.* **284,** 35572–35579
14. Mayans, O., Scott, M., Connerton, I., Gravesen, T., Benen, J., Visser, J.,

Pickersgill, R., and Jenkins, J. (1997) *Structure* **5,** 677–689

15. Abbott, D. W., and Boraston, A. B. (2007) *J. Biol. Chem.* **282,** 35328–35336
16. Creze, C., Castang, S., Derivery, E., Haser, R., Hugouvieux-Cotte-Pattat, N., Shevchik, V. E., and Gouet, P. (2008) *J. Biol. Chem.* **283,** 18260–18268
17. Charnock, S. J., Brown, I. E., Turkenburg, J. P., Black, G. W., and Davies, G. J. (2002) *Proc. Natl. Acad. Sci. U.S.A.* **99,** 12067–12072
18. Ogura, K., Yamasaki, M., Mikami, B., Hashimoto, W., and Murata, K. (2008) *J. Mol. Biol.* **380,** 373–385
19. Yoon, H.-J., Hashimoto, W., Miyake, O., Murata, K., and Mikami, B. (2001) *J. Mol. Biol.* **307,** 9–16
20. McDonough, M. A., Kadirvelraj, R., Harris, P., Poulsen, J. C., and Larsen, S. (2004) *FEBS Lett.* **565,** 188–194
21. Ochiai, A., Itoh, T., Maruyama, Y., Kawamata, A., Mikami, B., Hashimoto, W., and Murata, K. (2007) *J. Biol. Chem.* **282,** 37134–37145
22. Lunin, V. V., Li, Y., Linhardt, R. J., Miyazono, H., Kyogashima, M., Kaneko, T., Bell, A. W., and Cygler, M. (2004) *J. Mol. Biol.* **337,** 367–386
23. Rigden, D. J., and Jedrzejas, M. J. (2003) *J. Biol. Chem.* **278,** 50596–50606
24. Mishra, P., Prem Kumar, R., Ethayathulla, A. S., Singh, N., Sharma, S., Perbandt, M., Betzel, C., Kaur, P., Srinivasan, A., Bhakuni, V., and Singh, T. P. (2009) *FEBS J.* **276,** 3392–3402
25. Han, Y. H., Garron, M. L., Kim, H. Y., Kim, W. S., Zhang, Z., Ryu, K. S., Shaya, D., Xiao, Z., Cheong, C., Kim, Y. S., Linhardt, R. J., Jeon, Y. H., and Cygler, M. (2009) *J. Biol. Chem.* **284,** 34019–34027
26. Shaya, D., Tocilj, A., Li, Y., Myette, J., Venkataraman, G., Sasisekharan, R., and Cygler, M. (2006) *J. Biol. Chem.* **281,** 15525–15535
27. Weissbach, A., and Hurwitz, J. (1959) *J. Biol. Chem.* **234,** 705–709
28. Bradford, M. M. (1976) *Anal. Biochem.* **72,** 248–254
29. Doublié, S., and Carter, C. W. J. (1992) *Crystallization of Nucleic Acids and Proteins: A Practical Approach*, Oxford University Press, Oxford, UK
30. Ochiai, A., Yamasaki, M., Mikami, B., Hashimoto, W., and Murata, K. (2006) *Acta Crystallogr. Sect. F Struct. Biol. Cryst. Commun.* **62,** 486–488
31. Otwinowski, Z., and Minor, W. (1997) *Methods Enzymol.* **276,** 307–326
32. Terwilliger, T. C., and Berendzen, J. (1999) *Acta Crystallogr. D Biol. Crystallogr.* **55,** 849–861
33. Terwilliger, T. C. (2000) *Acta Crystallogr. D Biol. Crystallogr.* **56,** 965–972
34. Emsley, P., and Cowtan, K. (2004) *Acta Crystallogr. D Biol. Crystallogr.* **60,** 2126–2132
35. Collaborative. (1994) *Acta Crystallogr. D Biol. Crystallogr.* **50,** 760–763
36. Murshudov, G. N., Vagin, A. A., and Dodson, E. J. (1997) *Acta Crystallogr. D Biol. Crystallogr.* **53,** 240–255
37. Kabsch, W. (1976) *Acta Crystallogr. A* **32,** 922–923
38. Laskowski, R. A., MacArthur, M. W., Moss, D. S., and Thornton, J. M. (1993) *J. Appl. Crystallogr.* **26,** 283–291
39. DeLano, W. L. (2004) *The PyMOL Molecular Graphics System*, DeLano Scientific LLC, San Carlos, CA
40. Berman, H. M., Westbrook, J., Feng, Z., Gilliland, G., Bhat, T. N., Weissig, H., Shindyalov, I. N., and Bourne, P. E. (2000) *Nucleic Acids Res.* **28,** 235–242
41. Luzzati, V. (1952) *Acta Crystallogr.* **5,** 802–810
42. Lovell, S. C., Davis, I. W., Arendall, W. B., 3rd, de Bakker, P. I., Word, J. M., Prisant, M. G., Richardson, J. S., and Richardson, D. C. (2003) *Proteins* **50,** 437–450
43. Ramachandran, G. N., and Sasisekharan, V. (1968) *Adv. Protein Chem.* **23,** 283–438
44. Holm, L., and Sander, C. (1993) *J. Mol. Biol.* **233,** 123–138
45. Mello, L. V., De Groot, B. L., Li, S., and Jedrzejas, M. J. (2002) *J. Biol. Chem.* **277,** 36678–36688
46. Murzin, A. G., Brenner, S. E., Hubbard, T., and Chothia, C. (1995) *J. Mol. Biol.* **247,** 536–540
47. Jedrzejas, M. J., Mello, L. V., de Groot, B. L., and Li, S. (2002) *J. Biol. Chem.* **277,** 28287–28297
48. Davies, G. J., Wilson, K. S., and Henrissat, B. (1997) *Biochem. J.* **321,** 557–559
49. Linker, A., Meyer, K., and Hoffman, P. (1956) *J. Biol. Chem.* **219,** 13–25
50. Jenkins, J., Shevchik, V. E., Hugouvieux-Cotte-Pattat, N., and Pickersgill, R. W. (2004) *J. Biol. Chem.* **279,** 9139–9145
51. Ochiai, A., Itoh, T., Mikami, B., Hashimoto, W., and Murata, K. (2009) *J. Biol. Chem.* **284,** 10181–10189